Preparation and Characterization of Chiral Zerovalent Organoruthenium Aqua Complexes

Yasuyuki Ura,† Fumiaki Tsunawaki,† Kenji Wada,† Masashi Shiotsuki,† Teruyuki Kondo,† Syuhei Yamaguchi,‡ Hideki Masuda,‡ Atsushi Ohnishi,§ and Take-aki Mitsudo*,†

Department of Energy and Hydrocarbon Chemistry, Graduate School of Engineering, Kyoto University, Nishikyo-ku, Kyoto 615-8510, Japan, Department of Applied Chemistry, Faculty of Engineering, Nagoya Institute of Technology, Showa-ku, Nagoya 466-8555, Japan, and CPI Company, Life Science Development Center, Daicel Chemical Industries, Ltd., Tsukuba, Ibaraki 305-0841, Japan

Received August 2, 2005

Enantiopure organoruthenium aqua complexes, Ru(dppe)(dmfm)$_2$(H$_2$O) (**1**) [dmfm = dimethyl fumarate] and Ru(QUINAP)(dmfm)$_2$(H$_2$O) (**2**) [QUINAP = 1-(2-diphenylphosphino-1-naphthyl)isoquinoline], were prepared and the absolute structures were determined by X-ray crystallography. In the crystals of these complexes, the water molecule is captured in the chiral coordination environment assisted by two different hydrogen bonds; that is, a chiral center is generated on the coordinated oxygen of water. The behavior of the coordinated water in **1** and **2** was monitored by variable-temperature ^{1}H NMR measurement. At lower than −60 to −70 °C, the nonequivalency of the geminal protons in the coordinated water molecule was observed even in solution. On the basis of the VT NMR data and DFT study, the behavior of the coordinated water was discussed. Complex **1** reacts with ammonia to give Ru(dppe)(dmfm)$_2$(NH$_3$) (**4**), which is the first example of the isolated mononuclear Ru(0) ammonia complex. Complex **4** was reversibly converted into **1** by the reaction with water.

Introduction

Investigation of the behavior of a water molecule in organometallic aqua complexes is of great interest since it offers fundamental information useful for the metal complex-catalyzed organic synthesis in aqueous media or the reactions using H_2O as a reagent.[1] A large number of organometallic aqua complexes have been synthesized and investigated to date, some of which have chemically nonequivalent geminal protons of the coordinated H_2O connected to adjacent ligand(s) through intramolecular hydrogen bonding in the solid state, as revealed by their X-ray crystallography.[2−12] Such aqua complexes can be classified into either of the following categories: (A) complexes where either of the geminal protons is fixed by one intramolecular hydrogen bond;[2−11] (B) complexes where the water molecule is fixed by two intramolecular hydrogen bonds and stands in the chiral coordination site.[12] However, in solution the nonequivalency of the geminal protons is lost due to the vigorous motion of H_2O and/or the rapid exchange with external protons; therefore, to the best of our knowledge, intensive investigation of the nonequivalency in solution has not yet been successful.

We previously reported the synthesis of a racemic zerovalent ruthenium aqua complex, Ru(dppe)(dmfm)$_2$(H$_2$O) (**1**) [dppe = 1,2-bis(diphenylphosphino)ethane, dmfm = dimethyl fumarate], by reacting *rac*-Ru(η^6-cot)(dmfm)$_2$[13] [cot = 1,3,5-cyclooctatriene] with H_2O and dppe, where H_2O is captured in the chiral coordination environment (eq 1).[14] Complex **1** belongs to category B;

* To whom correspondence should be addressed. Phone: +81 75 383 2506. Fax: +81 75 383 2507. E-mail: mitsudo@scl.kyoto-u.ac.jp.
† Kyoto University.
‡ Nagoya Institute of Technology.
§ Daicel Chemical Industries, Ltd.

(1) For reviews, see: (a) Joó F. In *Catalysis by Metal Complexes: Aqueous Organometallic Catalysis 23*; James, B. R., P., van Leeuwen, W. N. M., Eds.; Kluwer Academic Publishers: Dordrecht, 2001; p 300. (b) Cornils, B.; Herrmann, W. A. In *Aqueous-Phase Organometallic Catalysis: Concept and Applications*, 2nd & rev. ed.; Wiley-VCH: Weinheim, Germany, 2004; p 750. (c) Koelle, U. *Coord. Chem. Rev.* **1994**, *135/136*, 623. (d) Li, C.-J.; Chan, T.-H. In *Organic Reactions in Aqueous Media*; John Wiley & Sons: New York, 1997; p 199. (e) Auge, J.; Beletskaya, I. P.; Cheprakov, A. V.; Fringuelli, F.; Gajewski, J. J.; Garner, P. P.; Grieco, P. A.; Kobayashi, S.; Lubineau, A.; Parker, D. T.; Piermatti, O.; Pizzo, F.; Quenau, Y. In *Organic Synthesis in Water*; Grieco, P. A., Ed.; Thomson Science: London, 1998; p 310. (f) Grundler, P. V.; Laurenczy, G.; Merbach, A. E. *Helv. Chim. Acta* **2001**, *84*, 2854.
(2) Zhao, Q.; Wang, X.; Fang, R.; Tiekink, E. R. T. *Acta Crystallogr.* **2003**, *E59*, m719.
(3) Hokelek, T.; Necefoglu, H. *Acta Crystallogr.* **1999**, *C55*, 545.
(4) Zhang, X.; Fan, C.; Wang, W.; Chen, C.; Liu, Q. *Acta Crystallogr.* **2002**, *E58*, m688.
(5) Fettouhi, M.; Khaled, M.; Waheed, A.; Golhen, S.; Ouahab, L.; Sutter, J.; Kahn, O. *Inorg. Chem.* **1999**, *38*, 3967.
(6) Cucciolito, M. E.; Panunzi, A.; Ruffo, F.; Albano, V. G.; Monari, M. *Organometallics* **1999**, *18*, 3482.
(7) Halfen, J. A.; Bodwin, J. J.; Pecoraro, V. L. *Inorg. Chem.* **1998**, *37*, 5416.
(8) Sobolev, A. N.; Miminoshvili, E. B.; Miminoshvili, K. E.; Sakvarelidze, T. N. *Acta Crystallogr.* **2003**, *E59*, m836.
(9) Koman, M.; Baloghova, Z.; Valigura, D. *Acta Crystallogr.* **1998**, *C54*, 1277.
(10) Clegg, W.; Straughan, B. P. *Acta Crystallogr.* **1989**, *C45*, 1992.
(11) Bailey, A.; Griffith, W. P.; Leung, D. W. C.; White, A. J. P.; Williams, D. J. *Polyhedron* **2004**, *23*, 2631.
(12) Kuznetsov, V. F.; Yap, G. P. A.; Alper, H. *Organometallics* **2001**, *20*, 1300.
(13) Mitsudo, T.; Suzuki, T.; Zhang, S.-W.; Imai, D.; Fujita, K.; Manabe, T.; Shiotsuki, M.; Watanabe, Y.; Wada, K.; Kondo, T. *J. Am. Chem. Soc.* **1999**, *121*, 1839.

10.1021/om050664n CCC: $30.25
Publication on Web 10/14/2005

the coordinated H_2O is bound by the two nonequivalent intramolecular hydrogen bonds, and thus the oxygen atom of H_2O becomes a chiral center. We report here the synthesis of enantiopure zerovalent organoruthenium aqua complexes and the successful observation of the nonequivalent geminal protons of the coordinated H_2O in solution. The detailed behavior of the coordinated H_2O and further reaction of **1** with ammonia will be discussed.

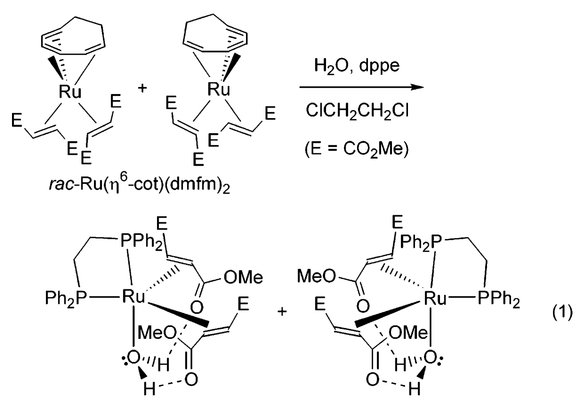

1a **1b**

Results and Discussion

Optical Resolution and Solid-State Structures of Enantiomeric Complexes 1a and 1b. The racemic aqua complex **1** was prepared as reported previously.[14] Spontaneous resolution of *rac*-**1**, which occurred during recrystallization from chlorobenzene/pentane, enabled the isolation of each enantiomer **1a** and **1b** in pure form. The solid-state structures of **1a** and **1b** determined by X-ray crystallography are shown in Figure 1, and their absolute configurations were confirmed by the values of the Flack parameters,[15] 0.00(4) for **1a** and 0.03(4) for **1b**, as refined by least-squares techniques. The water protons (H1, H2) could be found on the basis of Fourier maps. As clearly shown, the oxygen atom of H_2O (O1) is bound to ruthenium, and the two hydrogen atoms are located close to the carbonyl oxygen atoms of dimethyl fumarate ligands (O2, O3). The distances of O1···O2 (2.652(5) Å) and O1···O3 (2.643(5) Å) for **1a** and O1···O2 (2.657(6) Å) and O1···O3 (2.627(6) Å) for **1b** reflect the existence of intramolecular hydrogen bonds H1···O2 and H2···O3. The coordinative directions of the two dimethyl fumarate ligands differ from each other; in **1a** the dimethyl fumarate ligands coordinate to ruthenium by the (*re*, *re*)-enantioface, and in **1b** by the (*si*, *si*)-enantioface. Thus, the water protons H1 and H2 are fixed in different chemical environments, and a chiral center is generated on O1, in each enantiomer. Optical resolution of **1a** and **1b** by HPLC equipped with a chiral column was also successfully performed to give **1a** in 98% ee and **1b** in 92% ee. CD spectra of these separated complexes measured in $CHCl_3$ clearly showed an enantiomeric relation (Figure 2).

Synthesis and Solid-State Structure of Novel Zerovalent Ruthenium QUINAP Aqua Complex 2. By using an optically active P−N bidentate atropisomeric ligand, (*S*)-QUINAP [QUINAP = 1-(2-diphenylphosphino-1-naphthyl)isoquinoline],[16] instead of dppe, we obtained Ru((*S*)-QUINAP)(dmfm)$_2$(H_2O) (**2a**) in 29% yield as a single enantiomer (eq 2). However, fine single crystals suitable for X-ray analysis could not be obtained by recrystallization of **2a**. Further investigation revealed that *rac*-**2**, which was synthesized by the reaction of *rac*-Ru(η^6-cot)(dmfm)$_2$ with *rac*-QUINAP in the presence of H_2O, was successfully recrystallized from chlorobenzene/pentane to give fine yellow single crystals. The X-ray structure corresponding to the enantiomer **2a** is exhibited in Figure 3. The space group ($P2_1/n$) indicated that the crystals are racemic. Again, the water protons (H1, H2) were located on the basis of the Fourier map. Complex **2** also has a distorted trigonal bipyramidal structure like **1**. The phosphorus atom of QUINAP

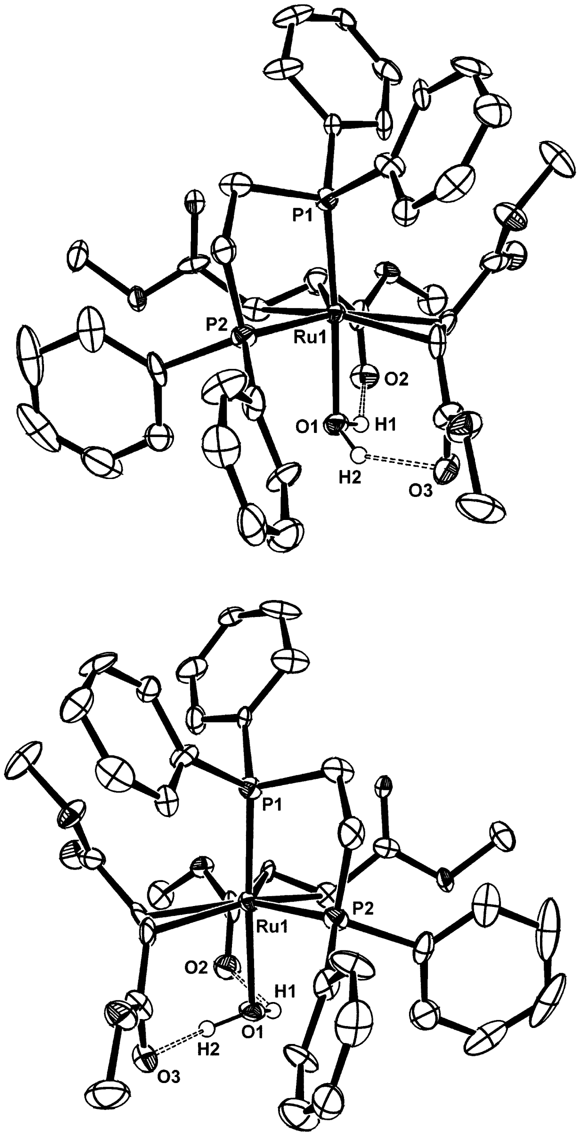

Figure 1. Molecular structures of **1a** (top) and **1b** (bottom). Thermal ellipsoids are set at 50% probability. Solvent and all hydrogen atoms except water are omitted for clarity. Dashed bonds between water protons (H1, H2) and oxygen atoms of dimethyl fumarates (O2, O3) exhibit hydrogen bonds.

(14) Shiotsuki, M.; Miyai, H.; Ura, Y.; Suzuki, T.; Kondo, T.; Mitsudo, T. *Organometallics* **2002**, *21*, 4960.
(15) Flack, H. D.; Bernardinelli, G. *J. Appl. Crystallogr.* **2000**, *33*, 1143.
(16) Lim, C. W.; Tissot, O.; Mattison, A.; Hooper, M. W.; Brown, J. M.; Cowley, A. R.; Hulmes, D. I.; Blacker, A. J. *Org. Process Res. Dev.* **2003**, *7*, 379.

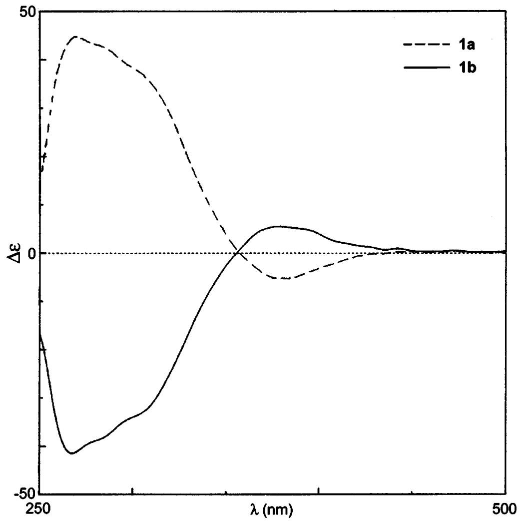

Figure 2. CD spectra of **1a** ($c = 2.5 \times 10^{-5}$ M) and **1b** ($c = 3.7 \times 10^{-5}$ M) in $CHCl_3$. For **1a**: λ_{max} 270 nm ($\Delta\epsilon$ +45), 381 (−5). For **1b**: λ 268 nm ($\Delta\epsilon$ −41), 378 (+5).

occupies an axial position and is *trans* to the water molecule, and the nitrogen atom is located at an equatorial position. The QUINAP ligand coordinates to ruthenium to avoid steric hindrance by the carbomethoxy groups of dimethyl fumarates located at equatorial positions. The distance O1−O2 (2.677(3) Å) is similar to those for **1a** and **1b**, while O1−O3 (2.581(3) Å) is slightly shorter, by ca. 0.04−0.06 Å.

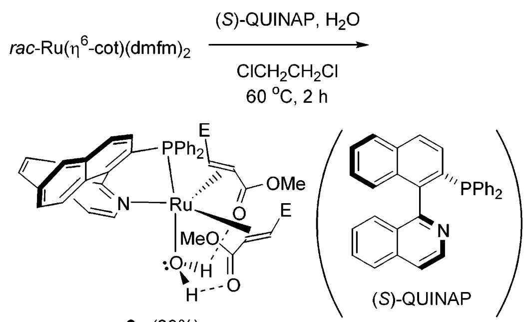

2a (29%)
(E = CO_2Me)

(2)

Variable-Temperature ^{1}H NMR Study of Complexes 1 and 2: Observation of the Nonequivalent Geminal Protons of the Coordinated H_2O and Their Positional Exchange in Solution. The behavior of H_2O in *rac*-**1** was examined by variable-temperature ^{1}H NMR spectroscopic analysis in CD_2Cl_2 (Figure 4a, left). The signal for the water protons appears as a broad singlet at 4.68 ppm at 25 °C. As the temperature was lowered, the broad singlet gradually sharpened (0 to −40 °C) with the appearance of a small shoulder peak at a slightly lower magnetic field, and the top of the signal began to split into two peaks at −70 °C. Further splitting was observed by cooling to −80 °C, with peaks at 4.64 and 4.52 ppm. This splitting indicates that the geminal protons of the coordinated H_2O are observed nonequivalently and their positional exchange is slowed by a decrease in temperature. The small shoulder peak observed below −40 °C may be due to the flip of the carbomethoxy group of the dmfm ligand. This flip can also be one possible reason for the broadening of the signal at 25 to ~0 °C as well as other factors such as an exchange of the water molecule with external ones, which will be discussed later.

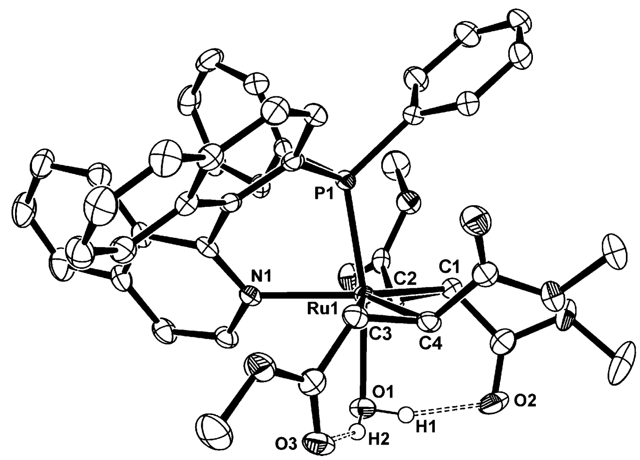

Figure 3. Molecular structure of **2** (the structure corresponding to **2a** is shown). Thermal ellipsoids are set at 50% probability. Solvent and all hydrogen atoms except water are omitted for clarity. Dashed bonds between water protons (H1, H2) and oxygen atoms of dimethyl fumarates (O2, O3) exhibit hydrogen bonds. Selected bond distances (Å) and angles (deg): Ru1−P1 = 2.2469(9), Ru1−O1 = 2.222(2), Ru1−C1 = 2.115(3), Ru1−C2 = 2.167(3), Ru1−C3 = 2.219(3), Ru1−C4 = 2.140(3), Ru1−N1 = 2.196(3), C1−C2 = 1.461(5), C3−C4 = 1.435(5), P1−Ru1−N1 = 81.17(7), O1−Ru1−N1 = 88.85(9), C1−Ru1−C4 = 90.6(1), C2−Ru1−N1 = 105.0(1), C3−Ru1−N1 = 86.7(1).

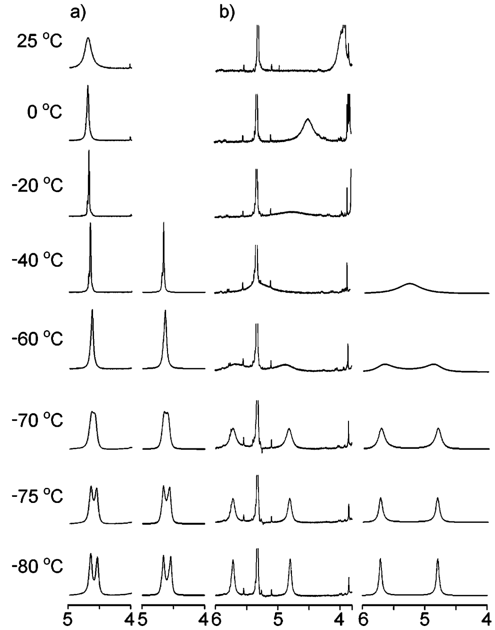

Figure 4. Experimental ^{1}H NMR spectra of **1** (a; left) and **2** (b; left) in CD_2Cl_2 at temperatures of 25 to −80 °C, and simulated ^{1}H NMR spectra of **1** (a; right) and **2** (b; right) at −40 to −80 °C. Chemical shifts are referenced to internal solvent resonances and reported relative to $SiMe_4$. The signal at 5.3 ppm in (b, left) derives from the solvent.

For *rac*-**2**, the ^{1}H NMR signal of the water protons appeared as a broad singlet at 3.98 ppm at 25 °C, overlapping with another peak (Figure 4b, left). The singlet peak comparatively shifted to lower magnetic field and broadened by cooling, in contrast to that of **1**. Two broad singlets appeared again at around 5.7 and 4.8 ppm at −60 °C, respectively, the shapes of which

Scheme 1. Possible Positional Exchange Process of the Water Protons via Rotation and Inversion

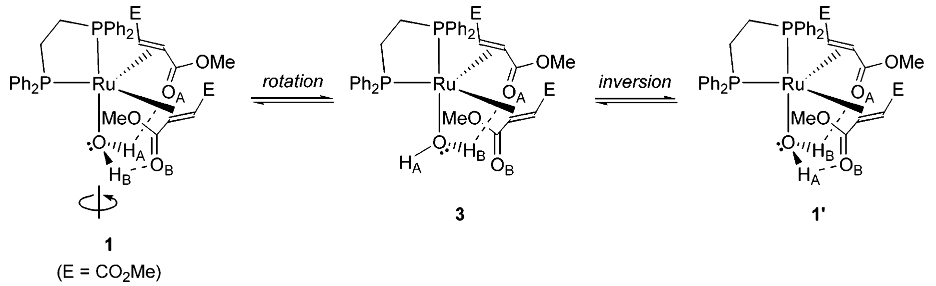

became sharper by further cooling to −80 °C. A $^{1}H-^{1}H$ COSY spectrum of **2** measured at −90 °C clearly showed the correlation between the two split singlets, revealing that these signals are assigned to the nonequivalent geminal protons of the identical water molecule (Figure 5).

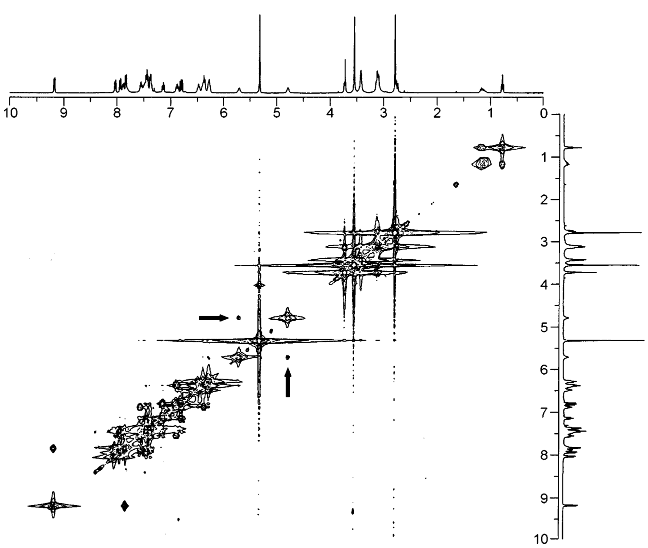

Figure 5. $^{1}H-^{1}H$ COSY spectrum of **2** measured at −90 °C. The correlation between the two split singlets of the water protons (5.71 and 4.79 ppm) can be observed clearly (indicated by arrows).

Line-shape analysis of the ^{1}H NMR spectra measured at −40 to −80 °C for **1** and **2** was performed by computer simulation (Figure 4a and 4b, right). The obtained activation parameters based on the Eyring plot were $\Delta H^{\ddagger} = 10.8$ kcal mol^{-1} and $\Delta S^{\ddagger} = 4.3$ cal mol^{-1} K^{-1} for **1** and $\Delta H^{\ddagger} = 7.5$ kcal mol^{-1} and $\Delta S^{\ddagger} = -10.9$ cal mol^{-1} K^{-1} for **2**. The slightly positive $\Delta S^{\ddagger}$ value for **1** indicates that the positional exchange of water protons occurs in an intramolecular manner. On the other hand, the negative $\Delta S^{\ddagger}$ value for **2** implies that another molecule such as a solvent (CD_2Cl_2) may participate in the transition state to lower the energy barrier. This exchange occurs even at −80 °C at a rate of ~30 Hz for **1** and ~50 Hz for **2**.

It is assumed that this process proceeds via both the rotation of H_2O around the Ru−O axis and the inversion (Scheme 1). The rotation by ~120° occurs to give the intermediate **3**, along with the dissociation of the hydrogen bonds $H_A\cdots O_A$ and $H_B\cdots O_B$ and the formation of a new hydrogen bond $H_B\cdots O_A$. The inversion of H_2O along with the formation of another hydrogen bond $H_A\cdots O_B$ completes the intramolecular positional exchange of the water protons. The dissociation/recoordination of the water molecule can also explain the positional exchange of the water protons,[17] whereas it seems to be unlikely (vide infra).

Density Functional Study on the Positional Exchange Process of the Water Protons: (a) Water Rotation and Inversion. On the basis of the assumption depicted in Scheme 1, the exchange process was investigated theoretically by the DFT method. Ru(dmpe)(dmfm)$_2$(H_2O) (**A**) [dmpe = 1,2-bis(dimethylphosphino)ethane] was used as a model complex. The geometries of complex **A**, intermediate **B** (corresponding to **3** in Scheme 1), and transition states for the rotation (**TS**$_{rot}$) and the inversion (**TS**$_{inv}$) were optimized by the B3LYP method with the basis set composed of the combination of SDD for Ru, the 6-31G(d,p) basis set for all oxygen and phosphorus atoms as well as two hydrogen atoms of coordinated water, and the 6-31G basis set for all other hydrogen and carbon atoms (see Experimental Section for details). The energetic profile and the optimized structures for **A**, **B**, **TS**$_{rot}$, and **TS**$_{inv}$ are exhibited in Figure 6. The upper structures correspond to the side views, and the lower ones the bottom views.

The geometries around the coordinated H_2O for **A**, **TS**$_{rot}$, **B**, and **TS**$_{inv}$ are shown in Figure 7. As H_2O in **A** rotates clockwise on the Ru1−O1 axis, both hydrogen bonds are weakened gradually, and in **TS**$_{rot}$, the original O3···H2 hydrogen bond is greatly lengthened. At this stage, the O1···O3 distance (2.856 Å) is longer by ca. 0.2 Å than that in **A** (2.670 Å). Although the distance of O1···O2 also becomes slightly longer (2.713 Å) than that in **A** (2.626 Å), the angle of H1−O1−H2 is considerably smaller than that in **A**. The theoretical energy barrier for the water rotation (13.6 kcal mol^{-1} based on ΔE_0) is moderately consistent with the activation enthalpy for **1** obtained experimentally (10.8 kcal mol^{-1}). Another rotation barrier, **TS**$_{rot}$′ (counterclockwise direction), is slightly higher than **TS**$_{rot}$, 15.5 kcal mol^{-1}, because of the cleavage of the stronger hydrogen bond O2···H1. In the next step from **TS**$_{rot}$ to the intermediate **B**, complete loss of the hydrogen bonds O3···H2 and O2···H1 occurs; instead, a new strong hydrogen bond O2···H2 is formed. The distance of O1···O3 (3.010 Å), where no hydrogen bond exists, is further lengthened by 0.15 Å than that in **TS**$_{rot}$. The hydrogen bond O2···H2 formed in **B** is maintained in **TS**$_{inv}$. The position of H1 is somewhat shifted to be close to the carbonyl oxygen O3; thus, the distance of O3···H1 in **TS**$_{inv}$ is fairly shorter than that in **B**. The O1···O3 distance is also shortened from 3.010 to 2.933 Å. The angles around the water molecule (H1−O1−H2, Ru1−O1−H1, and Ru1−O1−H2) are all increased by

(17) Helm, L.; Merbach, A. E. *Chem. Rev.* **2005**, *105*, 1923.

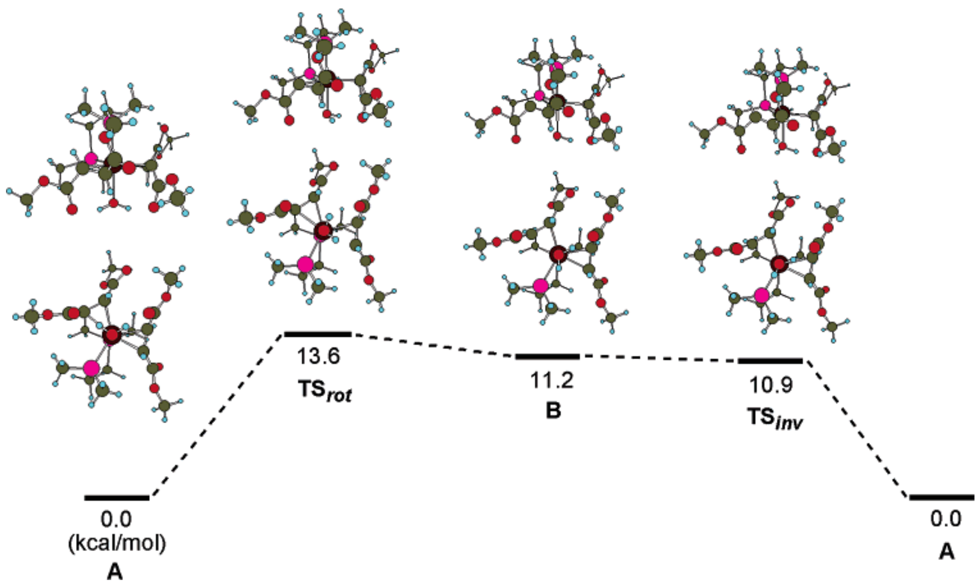

Figure 6. Energetic profile for the positional exchange of water protons via rotation and inversion.

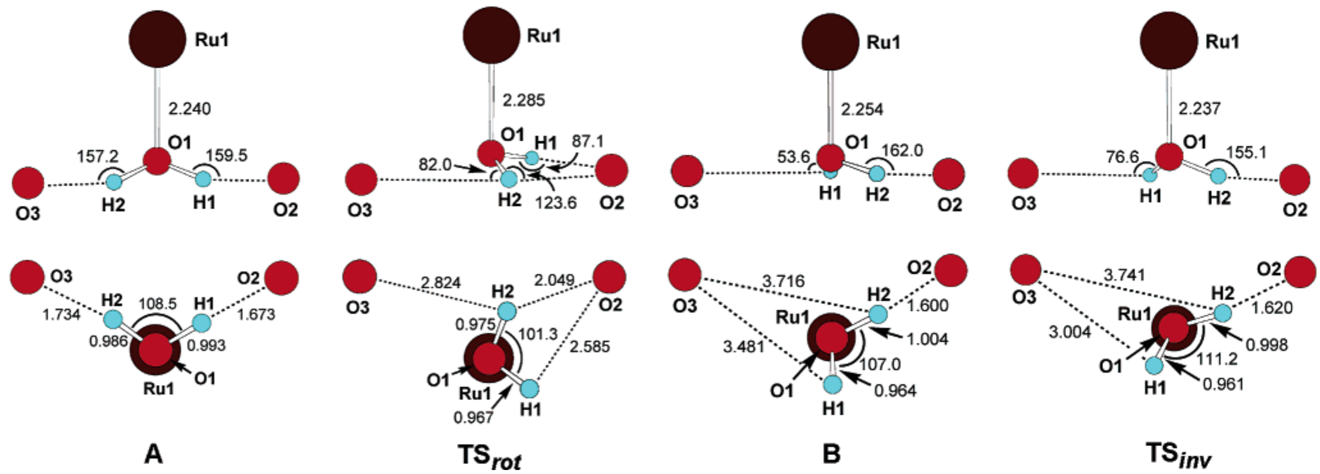

Figure 7. Simplified side and bottom views for **A**, **TS**$_{rot}$, **B**, and **TS**$_{inv}$. Selected bond distances (Å) and angles (deg) are shown.

4−10° in **TS**$_{inv}$ (111.2°, 124.7°, and 108.0°) compared with those in **B** (107.0°, 115.0°, and 103.2°). The Ru−OH_2 moiety in **TS**$_{inv}$ has an intermediate structure between pyramidal and trigonal planar, and the inversion from **B** to **A** seems to proceed smoothly with nearly no barrier.

(b) Possibility for the Exchange of the Coordinated H_2O with an External H_2O. As alternative mechanisms for the positional exchange of the water protons, dissociative and associative exchange of the coordinated H_2O with an external one can be considered. The dissociation of H_2O from **A** affords a coordinatively unsaturated 16-electron species, Ru(dmpe)(η^2-dmfm)$_2$, which is more thermodynamically unstable by 30.8 kcal mol^{-1} than **A** according to the calculation. A coordinatively saturated isomer of Ru(dmpe)(η^2-dmfm)$_2$, where a carbonyl oxygen atom of dmfm occupies the coordination site, was also calculated to be considerably more unstable than **A**, by 29.4 kcal mol^{-1}. These values are fairly greater than the observed $\Delta H^{\ddagger}$ for **1** and **2** obtained by the line-shape analysis. Judging from the observed $\Delta S^{\ddagger}$, both the dissociative and associative mechanisms are unlikely below −40 °C. DFT calculations at the B3LYP/LANL2DZ level show that the energy barrier of the associative pathway for **A** is ca. 18 kcal mol^{-1}, still somewhat greater than the experimentally obtained $\Delta H^{\ddagger}$ for **1** and **2**.

(c) Flipping Motion of the Carbomethoxy Groups. The flip of the carbomethoxy groups of dmfm ligands having hydrogen bonds with the water protons was also theoretically investigated. By rotating one of the carbomethoxy groups by ca. 180° to have a hydrogen bond between the water proton and the methoxy oxygen atom, the formed complexes were destabilized by 2.6−5.8 kcal mol^{-1}, and the rotation barriers were estimated to be 13.4−17.8 kcal mol^{-1}. The aqua complex having hydrogen bonds with both methoxy oxygen atoms was unstable by 8.9 kcal mol^{-1} compared with the stable structure of complex **A**.

Reaction of Aqua Complex 1 with Ammonia. The coordinated H_2O in **1** has been found to be labile. For example, the reaction of **1** with 1 atm of CO dissociates the water;[14] the amount of the liberated water was exactly determined by the Karl Fischer method,[18] and 85% of the theoretical amount of water was detected. Further investigations on the reactivity of **1** were

(18) Scholz, E. *Karl Fischer Titration*; Springer-Verlag: Berlin, 1984.

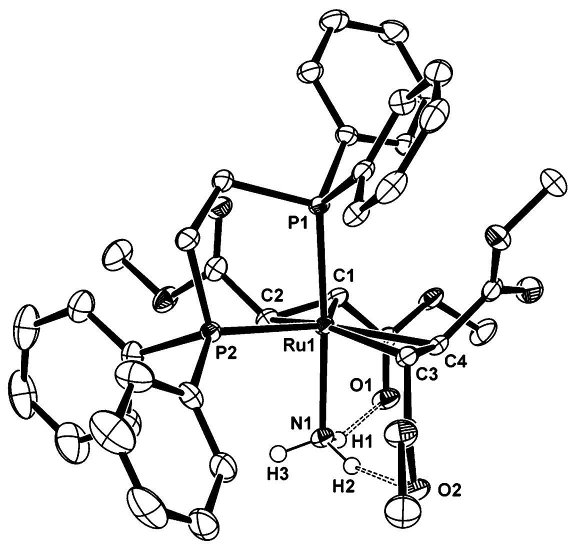

Figure 8. Molecular structure of **4** (the structure corresponding to **4a** is shown). Thermal ellipsoids are set at 50% probability. Solvent and all hydrogen atoms except ammonia are omitted for clarity. Dashed bonds between ammonia protons (H1, H2) and oxygen atoms of dimethyl fumarates (O1, O2) exhibit hydrogen bonds. Selected bond distances (Å) and angles (deg): Ru1−P1 = 2.3064(9), Ru1−P2 = 2.3841(9), Ru1−C1 = 2.150(3), Ru1−C2 = 2.192(3), Ru1−C3 = 2.212(3), Ru1−C4 = 2.152(3), Ru1−N1 = 2.200(3), C1−C2 = 1.440(5), C3−C4 = 1.445(5), P1−Ru1−P2 = 82.54(3), P2−Ru1−N1 = 94.13(8), P2−Ru1−C2 = 89.91(9), P2−Ru1−C3 = 102.71(9), C1−Ru1−C4 = 92.1(1).

carried out, where displacement of the water moiety was expected. Among the small polar molecules, ammonia in dioxane readily reacted with *rac*-**1** at ambient temperature (eq 3). After removal of the solvent, a green solid of a novel ammonia complex, *rac*-Ru(dppe)(dmfm)$_2$(NH_3) (**4**), was obtained in 88% isolated yield, and the single crystals were obtained by recrystallization from chloroform/pentane as racemates (the space group was $P\bar{1}$). The X-ray structure is shown in Figure 8. Complex **4** is the first example of the isolated mononuclear Ru(0) ammonia complex, whereas a large number of Ru ammonia complexes in higher oxidation states have been reported so far. Low-valent transition metal ammonia complexes are intriguing, since oxidative addition of ammonia may take place to afford amido hydride complexes.[19] In **4**, a chiral center is generated on the nitrogen atom of the coordinated NH_3.

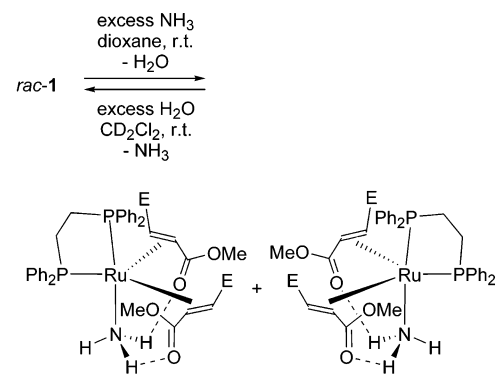

(3)

4a **4b**

The distances N1−O1 (2.791(3) Å) and N1−O2 (2.815(2) Å) are longer than the corresponding ones in aqua complexes **1** and **2** by ca. 0.13−0.19 Å. Although a low-temperature ^{1}H NMR measurement of **4** was also performed, no clear peak splitting of the ammonia protons was observed even at −90 °C. The calculated energy barrier for ammonia rotation in Ru(dmpe)(dmfm)$_2$(NH_3) is 4.6 kcal mol^{-1}, which is lower than that for the water rotation by 9.0 kcal mol^{-1}. These results are all consistent with decrease of the binding energy of the hydrogen bonds, compared with those in **1** and **2**. The ligand displacement reaction shown in eq 3 was revealed to be reversible by the NMR spectra; that is, complex **4** readily reacts with an excess amount of water to afford aqua complex **1** again.

Conclusion

Enantiopure organoruthenium aqua complexes **1a**, **1b**, and **2a** were synthesized, and the nonequivalent geminal protons of the coordinated H_2O in solution were successfully observed. The positional exchange of the geminal protons was strongly suggested to involve the rotation and inversion of H_2O by DFT calculation; the rotation has a higher energy barrier and the value was moderately consistent with that of the activated enthalpy obtained experimentally, and the inversion proceeded very smoothly. The Ru(0) ammonia complex **4** was successfully synthesized by reacting **1** with ammonia, and the energy barrier for the ammonia rotation was calculated, which was fairly lower than that for the water rotation. The information obtained here would assist in understanding the behavior of water molecules in general organometal aqua complexes, which leads to the development of the chemistry of water and related fields.

Experimental Section

General Methods. All manipulations were performed in an argon atmosphere using standard Schlenk techniques. Racemic complex **1** was prepared by the reported procedure.[14] All solvents were distilled under argon over appropriate drying reagents (sodium, calcium hydride, sodium-benzophenone, and calcium chloride). NMR spectra were recorded on JEOL EX-400 (FT, 400 MHz (^{1}H), 100 MHz (^{13}C), 162 MHz (^{31}P)) spectrometers. Chemical shift values (δ) for ^{1}H and ^{13}C are referenced to internal solvent resonances and reported relative to $SiMe_4$. Chemical shifts for ^{31}P are referenced to an external $P(OMe)_3$ resonance and reported relative to H_3PO_4. IR spectra were recorded on a Nicolet Impact 410 FT-IR spectrometer. Melting points were determined under argon on a Yanagimoto micro melting point apparatus. HR-MS spectra were recorded on JEOL SX102A spectrometers with *m*-nitrobenzyl alcohol (*m*-NBA) as a matrix. Elemental analyses were performed at the Microanalytical Center of Kyoto University. Circular dichroism spectra were recorded on a JASCO J-750 spectropolarimeter.

Spontaneous Resolution of Aqua Complex 1. Racemic complex **1** (ca. 3 mg) was dissolved in chlorobenzene (ca. 0.3 mL), and pentane (5 mL) was placed on the chlorobenzene solution. After 1 day, several crystals were formed. Unfortunately each enantiomer could not be separated even under microscope. Some of the crystals were confirmed to be **1a** and others were **1b**, respectively, by means of X-ray crystallography.

(19) (a) Zhao, J.; Goldman, A. S.; Hartwig, J. F. *Science* **2005**, *307*, 1080. (b) Casalnuovo, A. L.; Calabrese, J. C.; Milstein, D. *Inorg. Chem.* **1987**, *26*, 971. (c) Hillhouse, G. L.; Bercaw, J. E. *J. Am. Chem. Soc.* **1984**, *106*, 5472. (d) Bryan, E. G.; Johnson, B. F. G.; Lewis, J. *J. Chem. Soc., Dalton Trans.* **1977**, 1328.

Optical Resolution of 1. Racemic complex **1** (20 mg) was dissolved in chloroform (1 mL), and 2 mL of a hexane/acetone/THF mixture (85/10/5) was added. The solution was injected in four portions into a chiral column (CHIRALPAK IA, Daicel Chemical Industry, ϕ 2.0 × 25 cm). Elution with a mixture of hexane/acetone/THF (85/10/5) and subsequent evaporation of the obtained fractions and drying under vacuum afforded enantiomers **1a** (7 mg) in 98% ee and **1b** (6 mg) in 92% ee.

Preparation of Aqua Complex 2. Ru(η^6-cot)(dmfm)$_2$ (1.07 g, 2.16 mmol)[13] in distilled 1,2-dichloroethane (6 mL)/H_2O (9 mL) solution was stirred at 60 °C for 1 h. *rac*-QUINAP (952 mg, 2.16 mmol)[16] in distilled 1,2-dichloroethane (10 mL) was then added dropwise, and the mixture was stirred at 60 °C for 2 h. After the solvent and water were evaporated, the residue was dissolved in distilled chloroform and then chromatographed on alumina (ϕ 2.0 × 30 cm, Merck No. 1.01097, activity II−III). Elution with chloroform gave an orange solution, from which the solvent was evaporated. The brown residue was dissolved in chloroform (6 mL), and then pentane (150 mL) was added. The resulting orange precipitate was collected by filtration, washed with pentane (10 mL × 2), and dried under vacuum to give **2** (704 mg, 0.83 mmol, 38%).

Ru(*rac*-QUINAP)(dmfm)$_2$(H$_2$O) (2). Mp: 129−131 °C (dec). IR (KBr disk): 3058, 2949, 1691, 1655, 1433, 1317, 1172 cm^{-1}. ^{1}H NMR (400 MHz, CD_2Cl_2): δ 9.20 (d, 1H, J = 6.3 Hz), 7.94 (d, 1H, J = 8.3 Hz) 7.87 (d, 1H, J = 7.8 Hz), 7.78 (d, 1H, J = 7.8 Hz), 7.66 (d, 1H, J = 6.3 Hz), 7.62 (d, 1H, J = 8.3 Hz), 7.52−7.47 (m, 3H), 7.40−7.27 (m, 4H), 7.08 (dt, 1H, J = 1.0, 7.8 Hz) 6.95 (t, 1H, J = 7.8 Hz), 6.79 (d, 1H, J = 7.8 Hz), 6.62 (d, 1H, J = 8.3 Hz), 6.54 (d, 1H, J = 8.0 Hz), 6.52 (d, 1H, J = 8.0 Hz), 6.48 (t, 1H, J = 7.6 Hz), 6.30 (t, 2H, J = 7.6 Hz), 4.99 (br s, 2H, H_2O), 3.95 (d, 1H, J = 9.8 Hz, CH of dmfm), 3.73 (dd, 1H, J = 3.2, 9.5 Hz, CH of dmfm), 3.69 (s, 3H, OCH_3 of dmfm), 3.60 (s, 3H, OCH_3 of dmfm), 3.31 (s, 3H, OCH_3 of dmfm), 2.95 (d, 1H, J = 9.8 Hz, CH of dmfm), 2.90 (s, 3H, OCH_3 of dmfm), 2.73 (dd, 1H, J = 1.5, 9.3 Hz, CH of dmfm). ^{13}C NMR (100 MHz, CD_2Cl_2): δ 178.9 (C=O, 2C), 178.6 (C=O, 2C), 162.8, 148.4, 139.5, 139.0, 137.9 (d, J = 13.3 Hz), 136.0, 135.8, 135.7, 134.6 (d, J = 9.2 Hz), 133.8, 133.4 (d, J = 7.4 Hz), 133.3, 133.2, 131.2, 130.1, 129.7, 128.9 (2C), 128.4, 128.1, 127.6 (2C), 127.5, 127.3, 126.6 (2C), 126.2, 126.1, 126.0, 124.5, 120.2, 52.9 (s, =CH), 52.3 (d, J = 2.5 Hz, =CH), 51.4 (OMe), 51.3 (OMe), 50.9 (d, J = 4.2 Hz, =CH), 50.8 (OMe), 50.5 (OMe), 42.8 (s, =CH). ^{31}P NMR (162 MHz, CD_2Cl_2): δ 63.0. HR-MS(FAB-*m*NBA): *m/z* 847.1497, calcd for $C_{43}H_{40}NO_9PRu$ 847.1484. Anal. Calcd for $C_{43}H_{40}NO_9PRu$: C, 60.99; H, 4.76; N, 1.65. Found: C, 60.82; H, 4.78; N, 1.42.

Complex **2a** was prepared by a manner similar to that for **2**. In place of *rac*-QUINAP, (*s*)-QUINAP was used to give **2a** in 29% yield.

Preparation of Ammonia Complex 4. Complex **1** (80 mg, 0.10 mmol) was reacted with 0.5 M NH_3 in dioxane (4.0 mL, 2.0 mmol) at room temperature for 12 h. The color of the solution changed from yellow to green during the course of the reaction. Removal of the solvent followed by recrystallization from chloroform/pentane afforded green microcrystals (79 mg, 0.088 mmol, 88%).

Ru(dppe)(dmfm)$_2$(NH$_3$) (4). Mp: 147−151 °C (dec). IR (KBr disk): 3047, 2944, 1701, 1683, 1647, 1434, 1314, 1165 cm^{-1}. ^{1}H NMR (400 MHz, CD_2Cl_2): δ 7.51−7.31 (m, 15H), 7.08−7.23 (m, 3H), 6.82 (t, 2H, J = 8.8 Hz), 3.75−3.80 (m, 1H, CH of dmfm), 3.77 (s, 3H, OCH_3 of dmfm), 3.54 (s, 3H, OCH_3 of dmfm), 3.19 (s, 3H, OCH_3 of dmfm), 3.08 (ddd, 1H, J = 1.0, 2.9, 4.9 Hz, CH of dmfm), 2.95 (s, 3H, OCH_3 of dmfm), 2.72−2.84 (m, 2H, CH_2 of PCH_2), 2.13−2.27 (m, 4H, CH_2 of PCH_2 and CH of dmfm), 1.93 (br s, 3H, NH_3). ^{13}C NMR (100 MHz, CD_2Cl_2): δ 181.2 (d, C=O, J = 5.0 Hz), 180.6 (C=O), 180.4 (d, C=O, J = 2.5 Hz), 177.9 (d, C=O, J = 5.8 Hz), 139.6 (d, J = 30.0 Hz), 138.7 (d, J = 30.0 Hz), 138.5, 138.1, 133.7, 133.7, 132.7, 132.6, 131.3, 131.2, 129.9, 129.8, 129.6 (d, J = 1.7 Hz), 129.5 (d, J = 1.7 Hz), 129.0, 128.9, 128.8, 128.8, 128.8, 128.3 (d, J = 2.5 Hz), 127.7, 127.7, 127.1, 127.1, 51.4 (OMe), 51.4 (OMe), 51.1 (OMe), 51.0 (dd, J = 1.7, 6.7 Hz, CH of dmfm), 50.7 (OMe), 49.1 (dd, CH of dmfm, J = 2.5, 10.0 Hz), 46.6 (dd, CH of dmfm, J = 1.7, 5.8 Hz), 45.0 (dd, olefin of dmfm, J = 2.5, 3.3 Hz), 29.3 (dd, PCH_2, J = 18.8, 13.3 Hz), 23.7 (dd, PCH_2, J = 9.2, 19.2 Hz). ^{31}P NMR (162 MHz, CD_2Cl_2): δ 61.2, 45.5. Anal. Calcd for $C_{38}H_{43}NO_8P_2Ru{\cdot}0.5CHCl_3$: C, 53.49; H, 5.07; N, 1.62. Found: C, 53.39; H, 5.09; N, 1.32.

Crystallographic Study for 1a, 1b, 2, and 4. Crystals stable for X-ray diffraction measurements obtained by recrystallization from chlorobenzene/pentane were mounted on glass fibers. The diffraction data were collected with a Rigaku Mercury CCD area detector using graphite-monochromated Mo Kα radiation (λ = 0.71069 Å) with the oscillation technique. Crystal data and experimental details are listed in Table 1. All structures were solved by a combination of direct methods and Fourier techniques. Non-hydrogen atoms were anisotropically refined by full-matrix least squares calculations. Hydrogen atoms were located from the difference Fourier maps but not refined. Refinements were continued until all shifts were smaller than one-tenth of the standard deviations of the parameters involved. Atomic scattering factors and anomalous dispersion terms were taken from the International Tables for X-ray Crystallography.[20] All calculations were carried out with a Japan SGI workstation computer using the CrystalStructure crystallographic software package.[21,22]

Dynamic NMR Simulation for 1 and 2. The multispin dynamic NMR simulations were performed using the WinDNMR program package.[23] For complex **1**, the simulation pattern of 2×2-spin was selected, in which two independent sets of exchangeable protons, H_A−H_B and $H_{A'}$−$H_{B'}$, were considered. For both sets, the differences of chemical shifts of two exchangeable protons were set to be 41.5 Hz. Both sets of protons were postulated to be exchange at the same rate, k_{ab}. The exchange between H_A and $H_{A'}$ (or H_B and $H_{B'}$) was not considered at temperatures below −40 °C. The signal of the $H_{A'}$ (or $H_{B'}$) proton was located at the lower field than that of H_A (or H_B) by 11.5 Hz, and the ratio of H_A plus H_B versus $H_{A'}$ plus $H_{B'}$ protons was set to be 0.83/0.17. For complex **2**, the simple 2-spin simulation pattern was employed. The natural line width for each spectrum was determined on the basis of the measurement of nonexchanging peaks of the complexes.

Theoretical Calculations. To consistently compare the single-point energies of model complexes, calculations were carried out using density functional theory (DFT) optimized geometries. Calculations were performed using the Gaussian 03 RevB.04[24] implementation of B3LYP [Becke three-param-

(20) Ibers, J. A., Hamilton, W. C., Eds. *International Tables for X-ray Crystallography*; Kynoch Press: Birmingham, UK, 1974; Vol. IV.
(21) *CrystalStructure 3.6.0, Crystal Structure Analysis Package*; Rigaku and Rigaku/MSC, 2000−2004.
(22) Watkin, D. J.; Prout, C. K.; Carruthers, J. R.; Betteridge, P. W. *CRYSTALS Issue 10*; Chemical Crystallography Laboratory: Oxford, UK, 1996.
(23) Reich, H. J. *WinDNMR; Dynamic NMR Spectra for Windows J. Chem. Educ. Software* 3D2.
(24) Frisch, M. J.; Trucks, G. W.; Schlegel, H. B.; Scuseria, G. E.; Robb, M. A.; Cheeseman, J. R.; Montgomery, J. A., Jr.; Vreven, T.; Kudin, K. N.; Burant, J. C.; Millam, J. M.; Iyengar, S. S.; Tomasi, J.; Barone, V.; Mennucci, B.; Cossi, M.; Scalmani, G.; Rega, N.; Petersson, G. A.; Nakatsuji, H.; Hada, M.; Ehara, M.; Toyota, K.; Fukuda, R.; Hasegawa, J.; Ishida, M.; Nakajima, T.; Honda, Y.; Kitao, O.; Nakai, H.; Klene, M.; Li, X.; Knox, J. E.; Hratchian, H. P.; Cross, J. B.; Bakken, V.; Adamo, C.; Jaramillo, J.; Gomperts, R.; Stratmann, R. E.; Yazyev, O.; Austin, A. J.; Cammi, R.; Pomelli, C.; Ochterski, J. W.; Ayala, P. Y.; Morokuma, K.; Voth, G. A.; Salvador, P.; Dannenberg, J. J.; Zakrzewski, V. G.; Dapprich, S.; Daniels, A. D.; Strain, M. C.; Farkas, O.; Malick, D. K.; Rabuck, A. D.; Raghavachari, K.; Foresman, J. B.; Ortiz, J. V.; Cui, Q.; Baboul, A. G.; Clifford, S.; Cioslowski, J.; Stefanov, B. B.; Liu, G.; Liashenko, A.; Piskorz, P.; Komaromi, I.; Martin, R. L.; Fox, D. J.; Keith, T.; Al-Laham, M. A.; Peng, C. Y.; Nanayakkara, A.; Challacombe, M.; Gill, P. M. W.; Johnson, B.; Chen, W.; Wong, M. W.; Gonzalez, C.; Pople, J. A. *Gaussian 03*, revision B.04; Gaussian, Inc.: Pittsburgh, PA, 2003.

Table 1. Summary of Crystal Data, Collection Data, and Refinement of 1a, 1b, 2, and 4

	1a	**1b**	**2**	**4**
formula	$C_{38}H_{42}O_9P_2Ru{\cdot}C_6H_5Cl$	$C_{38}H_{42}O_9P_2Ru{\cdot}C_6H_5Cl$	$C_{43}H_{40}NO_9PRu{\cdot}C_6H_5Cl$	$C_{38}H_{43}NO_8P_2Ru{\cdot}0.5CHCl_3$
fw	918.32	918.32	959.39	864.47
cryst color	yellow	yellow	yellow	green
habit	platelet	platelet	platelet	block
cryst size, mm	0.20 × 0.10 × 0.05	0.10 × 0.10 × 0.05	0.35 × 0.20 × 0.05	0.50 × 0.25 × 0.10
cryst syst	orthorhombic	orthorhombic	monoclinic	triclinic
space group	$P2_12_12_1$ (#19)	$P2_12_12_1$ (#19)	$P2_1/n$ (#14)	$P\bar{1}$ (#2)
a, Å	8.9549(13)	8.947(2)	13.2604(4)	8.9268(4)
b, Å	12.856(2)	12.850(3)	23.9503(9)	11.6343(4)
c, Å	36.668(5)	36.617(7)	13.5294(5)	19.467(1)
α, deg	90	90	90	104.400(2)
β, deg	90	90	93.164(2)	100.860(2)
γ, deg	90	90	90	93.692(1)
V, Å^3	4221.2(11)	4209.7(14)	4290.3(3)	1910.0(2)
Z	4	4	4	2
D(calcd), g cm^{-3}	1.445	1.449	1.485	1.503
data collection temp, °C	−100	−100	−100	−130
μ(Mo Kα), cm^{-1}	5.65	5.67	5.25	6.52
$2\theta_{max}$, deg	55.0	55.0	55.0	54.7
no. of measd reflns	33 752	32 681	34 574	16 220
no. of unique reflns	9685 (R_{int} = 0.058)	9606 (R_{int} = 0.059)	9808 (R_{int} = 0.034)	8110 (R_{int} = 0.030)
no. of obsd reflns	5414 ($I > 2.00\sigma(I)$)	5062 ($I > 2.00\sigma(I)$)	5556 ($I > 3.00\sigma(I)$)	7035 ($I > 3.00\sigma(I)$)
no. of variables	484	530	612	530
R^a	0.033 ($I > 2.00\sigma(I)$)	0.038 ($I > 2.00\sigma(I)$)	0.031 ($I > 3.00\sigma(I)$)	0.040 ($I > 3.00\sigma(I)$)
$R_w{}^a$	0.042 ($I > 2.00\sigma(I)$)	0.043 ($I > 2.00\sigma(I)$)	0.030 ($I > 3.00\sigma(I)$)	0.118 ($I > 3.00\sigma(I)$)
GOF	1.052	1.09	1.00	1.190

^{a} $R = \sum||F_o| - |F_c||/\sum|F_o|$; $R_w = [\sum w(|F_o| - |F_c|)^2/\sum wF_o^2]^{1/2}$.

eter exchange functional (B3)[25] and the Lee−Yang−Parr correlation functional (LYP)[26] on Intel PIV computers at Kyoto University. The basis set composed of the combination of the Stuttgart−Dresden−Bonn energy-consistent pseudopotential (SDD)[27] for Ru, the 6-31G(d,p) basis set for all oxygen and phosphorus atoms as well as two hydrogen atoms of coordinated water, and the 6-31G basis set for all other hydrogen and carbon atoms were used. No constraints were imposed for all the systems. Frequency calculations on optimized species established that the energy minima possessed only real frequencies and the transition states possessed a single imaginary frequency. Zero-point energy and thermodynamic functions were computed at standard temperature (298.15 K) and pressure (1 atm). Spatial plots of the optimized geometries and frontier orbitals were obtained from Gaussian 03 output using Cambridge Soft Corporation's Chem 3D Pro v4.0 and Fujitsu WinMOPAC v3.5.

(25) Becke, A. D. *J. Chem. Phys.* **1993**, *98*, 5648.
(26) Lee, C.; Yang, W.; Parr, R. G. *Phys. Rev.* **1988**, *B37*, 785.
(27) Dolg, M. In *Modern Methods and Algorithms of Quantum Chemistry*; Grotendorst, J., Ed.; John von Neumann Institute for Computing: Zülich, 2000; Vol. 1, pp 479−508.

Acknowledgment. This work was supported in part by Grants-in-Aid for Scientific Research (A and B) and Scientific Research on Priority Areas from the Japan Society for the Promotion of Science and the Ministry of Education, Culture, Sports, Science and Technology, Japan. T.K. acknowledges financial support from the Sumitomo Foundation and Japan Chemical Innovation Institute. We thank Dr. M. Shiro (Rigaku Corp.) for supporting our X-ray crystallography.

Supporting Information Available: The results of the dynamic NMR simulation for **1** and **2** and the theoretical calculations. This material is available free of charge via the Internet at http://pubs.acs.org.

OM050664N